http://dx.doi.org/10.5012/bkcs.2013.34.6.1800

Chemoenzymatic Synthesis of Dual-responsive Amphiphilic Block Copolymers and Drug Release Studies

Peng Chen, Ya-Peng Li,* Shu-Wei Wang, Xin-Lei Meng, Ming Zhu, and Jing-Yuan Wang

*Alan G. MacDiarmid Institute of Jilin University, Changchun 130012, P.R. China. *E-mail: liyapeng@jlu.edu.cn*
Received December 3, 2012, Accepted March 24, 2013

Dual-responsive amphiphilic block copolymers were synthesized by combining enzymatic ring-opening polymerization (eROP) of ε-caprolactone (CL) and ATRP of *N,N*-dimethylamino-2-ethyl methacrylate (DMAEMA). The obtained block copolymers were characterized by gel permeation chromatography (GPC), ^{1}H NMR and FTIR-IR. The critical micelle concentration (CMC) of copolymer was determined by fluorescence spectra, it can be found that with hydrophilic block (PDMAEMA) increasing, CMC value of the polymer sample increased accordingly, and the CMC value was 0.012 mg/mL, 0.025 mg/mL and 0.037 mg/mL for PCL_{50}-*b*-$PDMAEMA_{68}$, PCL_{50}-*b*-$PDMAEMA_{89}$, PCL_{50}-*b*-$PDMAEMA_{112}$, PCL_{50}-*b*-$PDMAEMA_{89}$ was chosen as drug carrier to study in vitro release profile of anti-cancer drug (taxol). The temperature and pH dependence of the values of hydrodynamic diameter (Dh) of micelles, and self-assembly of the resulting block copolymers in water were evaluated by dynamic light scattering (DLS). The result showed that with the temperature increasing and pH decreasing, the Dh decreased. Drug-loaded nanoparticles were fabricated using paclitaxel as model. Transmission electron microscopy (TEM) and atomic force microscopy (AFM) had been explored to study the morphology of the hollow micelles and the nanoparticles, revealing well-dispersed spheres with the average diameters both around 80 nm. In vitro release kinetics of paclitaxel from the nanoparticles was also investigated in different conditions (pH and temperature, *etc*.), revealing that the drug release was triggered by temperature changes upon the lower critical solution temperature (LCST) at pH 7.4, and at 37 °C by an increase of pH.

Key Words : Stimuli-responsive polymers, Amphiphilic block copolymer, Chemoenzymatic synthesis, Drug release

Introduction

Stimuli-responsive amphiphilic block copolymers have recently attracted considerable attention due to their potential for biomedical and engineering application.[1-4] Changes of conformation and physical properties of the stimuli-sensitive component induced self-assembly of the block copolymers into micelle-like structures consisting of a hydrophobic core and a hydrophilic corona, which could serve as an efficient drug and gene delivery agent, and meanwhile could also prompt disassociation of polymeric micelles.[5-8] Synthetic block polymers in which each block possessed element responsive to different stimuli were extensively investigated. A typical example was poly(*N*-isopropyl acrylamide) (PNIPAAm)-based block copolymers, with pH-sensitive constituent beared as well, such as poly(4-vinyl pyridine) (P4VP), poly(acrylic acid) (PAAc), poly(sodium styrene sulfonate) (PSSNa), *etc*.[9-11] The emergence of multiple-responsive component, however, facilitated development of simply constructed smart systems, for example, Axel H. E. Müller and his coworkers synthesized star-shaped and linear poly(*N,N*-dimethylaminoethyl methacrylate) (PDMAEMA), and discussed the difference of the pH dependence of cloud point temperature between star-shaped PDMAEMA and their linear analogues.[12]

Biocatalysis allowed the successful transformations of a variety of small organic functional molecules and in the past a few years, was evaluated as an efficient way to enrich the chemical products.[13] *In vitro* enzyme catalysis, as a new environmentally friendly methodology, has been expanded to the polymer synthesis and modification. The green biocatalyst enzyme became a competitive candidacy in the catalytic chemistry field, apart from the traditional chemical organometallic catalyst,[14,15] most likely due to their non-toxicity, recyclability, (enatio-, regio- and chemo-) selectivity, biocompatibility and ability to operate without demanding conditions.[16,17] Now as polymer science advanced, biocatalytic approach has acted as a compelling choice for the synthesis of polymers with well-defined architectures, amongst which some would be beyond imagination when in the presence of conventional chemical catalysts.[18-20] Enzymatic polymerization methods, however, are detrimental to some special groups, which will narrow down their application on the synthesis of some functional polymers. To overcome the disadvantage, the development of mutually compatible chemo- and biocatalytic methods is required.

Novel polymerization techniques, *i.e*. living cationic polymerization,[21-23] living ionic polymerization,[24-26] and living/control radical polymerization,[27-29] allowed facile synthesis of well-defined amphiphilic block copolymers. Among those polymerization methods, living/control radical polymerization itself, especially atom transfer radical polymerization (ATRP)[30-32]

and reversible addition-fragmentation transfer polymerization (RAFT),[33,34] demonstrated remarkable superiority over other ways, leading to a noteworthy advance in the study of amphiphilic block copolymers, in particular, their unique supramolecular structure in aqueous solution and appealing characteristics relevant to biomedicine and bioengineering.[35-38] Whereas the combination of enzymatic ring-opening polymerization and ATRP, first reported by Andreas Heise, was virtually a simple and efficient route to prepare copolymers,[39] the architecture of which was comprised of hydrophilic blocks and hydrophobic blocks attached at the same joint.

Thus, the combination of eROP and ATRP has been one of the most promising techniques and a large number of functional polymers could be synthesized effectively. Our laboratories have reported the synthesis of block copolymers by the combination of eROP and ATRP, including AB-type block copolymers PCL-*b*-PSt, ABA-type block copolymers PSt-*b*-PCL-*b*-PSt and the pentablock copolymers PSt-*b*-PCL-*b*-PEG-*b*-PCL-*b*-PSt.[40-42]

In present study, we aim to construct dual-responsive amphiphilic block copolymers PCL-*b*-PDMAEMA by the combination of eROP and ATRP. The structures, molecular weight and molecular weight distribution of block copolymers were characterized by ^{1}H NMR, IR and GPC. The self-aggregation behavior of copolymers in water was investigated, and subsequently anti-cancer drug was encapsulated and its release profile from drug carrier was monitored systemically. The results showed that the drug release could be flexibly tuned by pH and temperature, and circulation time of PTX at higher pH and temperatures was prolonged conspicuously.

Experimental

Materials. Novozyme-435 (immobilized Candida Antarctica lipase B, specific activity 7000 PLU/g) was provided by Novozymes (Denmark). ε-caprolactone was purchased from Aldrich Chemical Co. and distilled over calcium hydride (CaH_2) under vacuum before use. Methanol (anhydrous, 99.8%) purchased from Aldrich Chemical Co. was directly used. *N,N*-Dimethylaminoethyl methacrylate was passed from base aluminium oxide to eliminate polymerization inhibitor and stored at −10 °C for use. Copper(I) chloride (CuCl, Beijing Chemical Co.) was purified by precipitation from acetic acid to remove Cu^{2+}, filtrated and washed with ethanol, and then dried. 2-Bromopropionyl bromide (97%) and hexamethyltriethylenetetramine (HMTETA) was purchased from Aldrich Chemical Co without further purification. Solvents were distilled over drying agents under nitrogen prior to use: methylene chloride (CH_2Cl_2) from calcium hydride, and tetrahydrofuran (THF) from sodium/benzophenone. Triethylamine (TEA, Beijing chemical Co.) was refluxed for 12 h in the presence of Ca_2H_2 and distilled under vacuum. All the reagents used in this study were of analytic grade.

Instruments. ^{1}H nuclear magnetic resonance (NMR) measurements were conducted on a Bruker ARX-500 NMR (500 MHz) spectrometer with $CDCl_3$ as solvent at room temperature. Chemical shifts (in parts per million, ppm) were reported downfield from 0.00 ppm using trimethylsilane (TMS) as internal standard. Molecular weights and molecular weight distributions were measured with a Waters 410 Gel permeation chromatography (GPC) apparatus equipped with a 10-μm Styragel HT6E column (300 mm × 7.8 mm) using linear polystyrene standards. THF was used as the eluent at a flow rate of 1 mL/min. The infrared spectra (IR) of polymers were recorded on a NICOLET Impact 410 at room temperature, using KBr pallet in the range of 400 to 4000 cm^{-1}. Dynamic laser scattering (DLS) measurements were performed on a laser light scattering spectrometer (BI-200 SM) equipped with equipped with an argon-ion laser (514 nm, 10.4 mW) at a given temperature, and the data analysis was based on a digital correlator (BI-9000 AT) software at the scattering angle of 90°. Atomic force microscopy (AFM) observations of the micelles absorbed on the freshly treated silicon wafer surface were carried out with the commercial instrument (Digital Instrument, Nanoscope IIIa, Multimode). All the tapping mode images were taken at room temperature in air with the microfabricated rectangle crystal silicon cantilevers (Nanosensor). The topography images were obtained at a resonance frequency of approximate 365 kHz for the probe oscillation. Photoluminescence (PL) spectra were recorded on a Jobin Yvon Spex Fluorolog 3 fluorescence spectrophotometer. Transmission electron microscopy (TEM) studies were performed with a JEOL JEM 2010 instrument operated at an accelerator voltage of 200 kV. Micelle solution was dropped onto a carbon-coated copper grid, followed by the removal of excess sample with filter paper, and then air dried prior to measurements. The concentration of the released paclitaxel in the dialysis media was determined by HPLC (Agilent 1100 Series).

Synthesis of Diblock Copolymers PCL-*b*-PDMAEMA. Novozyme-435 (0.216 g, 5% w/w of the monomer weight), dried over P_2O_5 in a vacuum desiccator (0.1 mm Hg, 25 °C) for 24 h, was transferred into an oven-dried 50 mL vial equipped with a magnetic bar under an argon atmosphere. The pre-degassed monomer caprolactone (4 mL, 37.8 mmol) and the solvent toluene (8.5 mL, twice the v/w ratio of the monomer) were added *via* a syringe under argon into the reaction vial, and then the initiator methanol (0.05 mL, 1.26 mmol) *via* microliter syringe. The vial was then placed into a constant temperature (70 °C) oil bath with magnetic stirring. After 6 h, reactions were terminated by pouring into excess cold chloroform and removing the enzyme by filtration. The residue on the filter was washed several times with hot chloroform. The filtrate was concentrated by rotary evaporation and precipitated at least in a 10-fold excess of methanol. The obtained product was dried overnight under vacuum.

PCL-OH (2 g, 0.204 mmol) was added into a two-neck flask which contained triethylamine (0.28 mL, 2.04 mmol) and 6 mL of dichloromethane, and then cooled in an ice bath (0 °C). After homogeneity was reached, to the flask was added dropwise 0.214 mL (2.04 mmol) of α-bromopropionyl

bromide in 5 mL of dry dichloromethane through the constant pressure dropping funnel. The reaction was carried out at 0 °C for 2 h and then transferred to room temperature for 22 h. The solution was filtrated to remove the quaternary ammonium halide $(CH_3CH_2)_3NH^+Br^-$. The filtrate was concentrated, and then precipitated and washed several times with excessive cold methanol. The product obtained after drying under vacuum overnight was collected, noted as macroinitiator.

Macroinitiator (0.035 g) and complex of CuCl (0.009 g, 0.09 mmol) and HMTETA (0.08 mL, 0.029 mmol) was added in an argon-purged flask. Three freeze-degas-thaw cycles was performed to remove oxygen from the reaction system. Monomer DMAEMA (2 mL) and solvent THF (1 mL) degassed by dry argon was introduced into the flask *via* an air-tight syringe. After the macroinitiator was completely dissolved, the reaction flask was immersed in an oil bath of 60 °C under sufficient stirring for 8 h. The reaction was terminated by exposure to air in a freezing condition. The solution was diluted with chloroform and passed through an alumina column for the removal of copper catalyst. The solution was concentrated by rotary evaporation and precipitated in hexane. The resulting products were dried under vacuum for 24 h, to yield white powder.

Samples Preparation for DLS AFM and TEM. The PCL-*b*-PDMAEMA was first dissolved in anhydrous THF (0.11 wt %) in a vial at room temperature. Drop addition of deionized water into the sonicated polymer solution was continued before turbidity appeared, which represented the formation of polymeric micelles, with about a pre-determined amount of water, at a volume ratio of 1/1 to THF consumed. The final volume of the mixture was adjusted to 25 mL by adding water into the vial. The solution was sonicated for another 1 h to allow the rapid diffusion of THF and water. To remove THF, the solution was dialyzed against 1.0 L distilled water for 48 h, during which the water was renewed every 12 h. The samples for AFM and TEM studies were prepared by drop-casting the micelle solution onto freshly cleaved silicon wafer surface and carbon-coated copper grid, respectively.

Critical Micelle Concentration (CMC). Pyrene was used as a hydrophobic fluorescent probe to determine the CMC owing to its preference of dwelling in the hydrophobic interior of the micelles. Aliquots of pyrene solutions (6×10^{-6} M in acetone, 1 mL) were added to volumetric flasks, and the acetone was evaporated in a vacuum oven for 24 h. 10 mL aqueous micellar solutions with different concentrations starting from a down to 1.0×10^{-6}, were added to these pyrene-contained flasks and allowed to equilibrate for 2 days prior to fluorescence measurement. Excitation spectra of fluorescent probe at serial concentrations of micellar solution were recorded from 350 to 500 nm, using an emission wavelength of 373 nm, from which the intensities of peaks at 339 nm and 335 nm could be evaluated. The CMC value of the polymer sample was determined through the plot of the ratio of the intensity of I_{339} to I_{335} vibronic bands against the log of the concentration of each polymeric solution, and specifically it means the intersection of two regression lines calculated from the linear regions of the graphs.

Encapsulation of Taxol by Polymeric Micelles. 100 mg of PCL-*b*-PDMAEMA was dissolved in 4 mL of THF, and then mixed with a solution of Taxol (40 mg) in DMF (2 mL). When the mixture turned into homogeneity after sonication, it was transferred into a treated dialysis bag (MWCO: 3000 Da) and subjected to dialysis against twice distilled water for 3 days at room temperature (refresh the water in 12 h). Filter (450 nm) was used to eliminate contaminants and large aggregates in emulsion, giving Taxol-loaded micelles as product.

***In vitro* Release of Taxol from Polymeric Micelles.** A series of phosphorous acid buffer solution (PBS) of varied concentrations were prepared, pH values of which were determined by acidometer. 1 mL of Taxol-loaded micelle solution was sealed within a treated dialysis bag that was then immersed in 9 mL of PBS solution with magnetic stirring at different temperatures. 8 mL of sample solution was taken at predetermined time intervals, with the same volume of fresh PBS solution added. The amount of Taxol in each sample was quantified through HPLC analysis, and accordingly, the percentage cumulative release could be obtained.

Results and Discussion

Synthesis of Diblock Copolymers PCL-*b*-PDMAEMA. Linear block copolymer has been researched heavily, while works about chemoenzymatic synthesis of block copolymers were not prevalently reported, up to now. As the extending

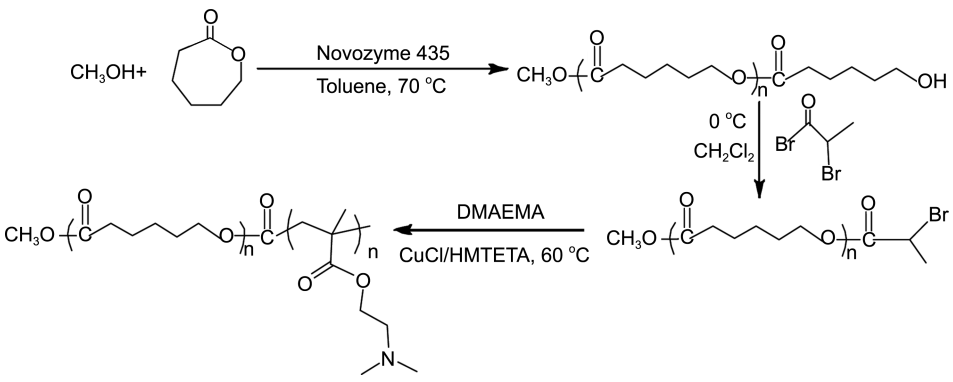

Scheme 1. Synthesis route of diblock polymer PCL-*b*-PDMAEMA.

of this technique, in this paper, we investigated the synthesis of diblock copolymer PCL-*b*-PDMAEMA by the combination of eROP of caprolactone and ATRP of methacrylate monomer. The general synthetic route for the preparation of the diblock copolymers is illustrated in Scheme 1. The advantages of this approach include: (1) all the processes don't need any demanding conditions; (2) all starting materials are inexpensive and readily available; (3) some laborious work or procedures can be cut down, like protecting group chemistry.

In the current study, methanol was used as initiators for the eROP step. Since water is also an effective initiator for eROP, possibility of competitive initiation between water and methanol would not be negligible. Hence to prepare pure methanol-initiated PCL, it is paramount to dry the reagents thoroughly, especially the biocatalyst Novozyme 435. A typical ^{1}H NMR spectrum of the resulting copolymer PCL-OH was shown in Figure 1(a). Besides the dominant PCL resonance signals at 1.4, 1.6, 2.3, and 4.1 ppm, the characteristic peak corresponding to methyl protons of initiator methanol, could be pointed out clearly at 3.68 ppm. The signal at 3.65 ppm corresponds to the methylene protons attached to the terminal hydroxyl group, which validated the successful initiation of ε-CL by methanol. The GPC analysis of PCL-OH showed a unimodal and symmetrical trace in Figure 2(a). It can be seen in Table 1 that number average molecular weight (Mn) of PCL-OH was 11293 g/mol and polydispersity was 1.36, respectively.

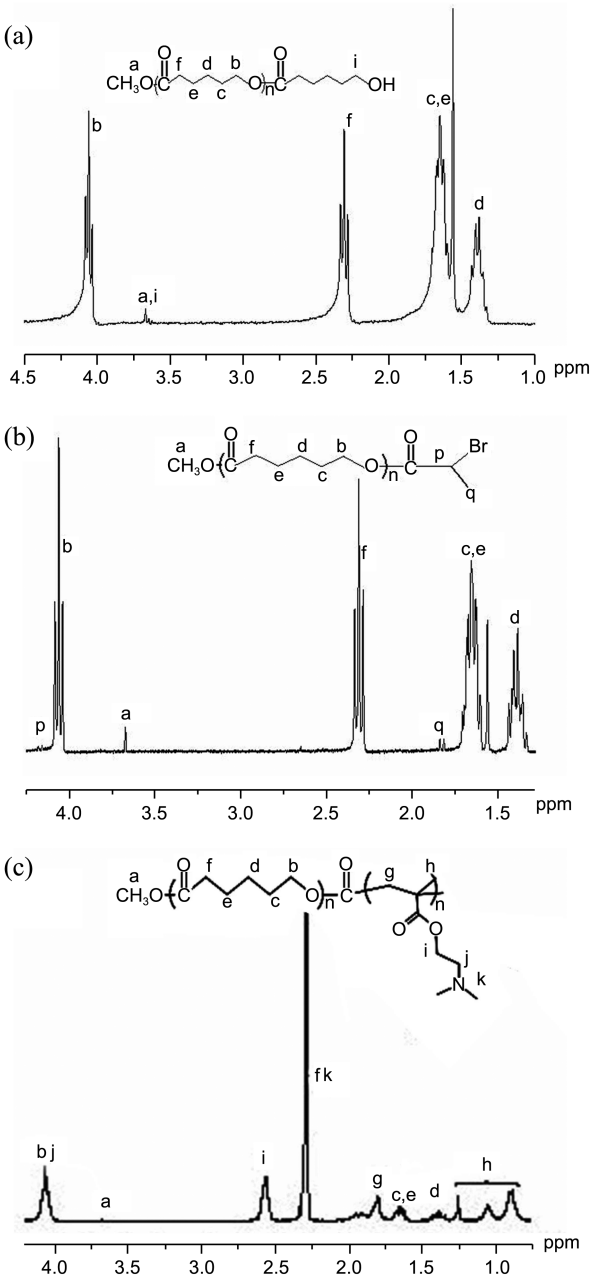

Figure 1. ^{1}H-NMR spectrum of PCL-OH (a), macroinitiator (b) and diblock copolymer PCL-*b*-PDMAEMA (c) were recorded at room temperature in $CDCl_3$.

Table 1. Results of PCL, Macroinitiator and block copolymers

		$Mn_{(th)}$[a]	$Mn_{(NMR)}$[b]	$Mn_{(CPC)}$[c]	Mw/Mn[c]
1	PCL-OH	3420	7800	11293	1.36
2	PCL-Br	11713	11352	12207	1.35
3	PCL-*b*-PDMAEMA	44572	48019	34506	1.30

[a]The theoretical molecular weights (Mn.th) calculated from the ratio of the initial monomer concentration to the initial initiator concentration $[M]_0/[I]_0$. [b]Determined by ^{1}H-NMR analysis. [c]Determined by GPC measurements.

The PCL-OH was converted to functional macroinitiator by esterification with 2-bromopropionyl bromide. To avoid cleavage of the polymer chains, the reaction was carried out at 0 °C in dried CH_2Cl_2 in the presence of TEA. The catalytic mechanism of TEA was to preticipate HCL from the solution in the form of quaternary ammonium halide $(CH_3CH_2)_3NH^+Br^-$, which favored the esterification. Figure 1(b) shows the ^{1}H NMR spectrum of the macroinitiator. The chemical shifts of methene protons and the methyl protons adjacent to the active bromide were identified at 4.23 ppm and 1.81 ppm, which confirmed that active halide-terminated (α-bromoester) macroinitiator was already constructed. Additionally, a narrow symmetrical GPC signal for macroinitiator was also observed in Figure 2(b), where the elution volume of macrointiator was found to increase, in consistence with a slightly increased molecular weight relative to polymer sample prior to esterification. However, the polydispersity index became dwindled, possibly resulting from inevitable fractionation of the macroinitiator during precipitation after esterification.

The ^{1}H NMR spectrum of copolymer depicted in Figure 1(c) clearly showed the characteristic signals of both the CL and DMAEMA units. The formation of the copolymers were verified through the characteristic resonances of OCH_2CH_2N and $N(CH_3)_2$ protons from the block of PDMAEMA at 2.58 ppm and 2.31 ppm, respectively, and those of methyl protons of $C(CH_3)$ from the same block at 1.21-0.80 ppm. The GPC curve in Figure 2(c) offered the information about molecular weight and molecular weight distribution. The result suggested that after the completion of ATRP of DMAEMA, the average number molecular weight of the copolymer was shifted to a high molecular weight region with the value of

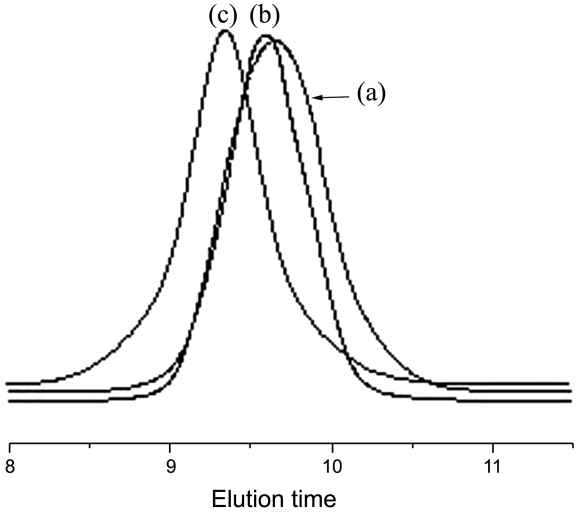

Figure 2. GPC traces of PCL-OH (a), macroinitiator PCL-Br (b) and diblock copolymer PCL-*b*-PDMAEMA (c). The molecular weight and polydispersity were determined by GPC.

34506 g/mol, and the value of polydispersity was 1.30, as shown in Table 1, which revealed the controlled nature of ATRP. That is to say, the block copolymer with a simultaneous thermo and pH sensitive PDMAEMA block was prepared successfully.

To further confirm the structure of copolymer, we utilized FT-IR measurement to characterize the block copolymer. Figure 3 exhibited the representative IR spectra of PCL-OH (a) and diblock copolymer PCL-*b*-PDMAEMA (b). After eROP of ε-CL, the occurrence of absorption band at 1734 cm^{-1} could be assigned to the stretching vibration of ester carbonyl group of the PCL blocks (Figure 3(a)). With subsequent ATRP of DMAEMA, all of the characteristic absorptions of PCL segments remained in the spectrum of the copolymer (Figure 3(b)), at the same time, the new peaks were found at 2776 and 2821 cm^{-1}, which belonged to the stretching vibration characteristic peaks for $-CH_3$ and $-CH_2-$ of PDMAEMA block. Two C-N stretching bands, new functional groups arising from the tertiary amine in DMAEMA, could be obviously discerned at 1274 and 1167 cm^{-1}. The variation in the IR spectra could be used as the indicative of successful preparation of the copolymer.

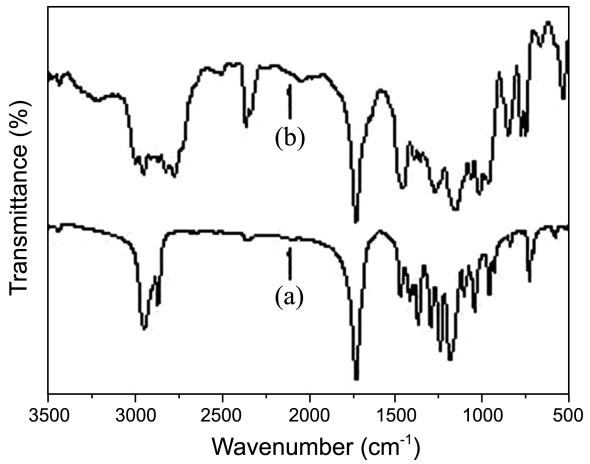

Figure 3. IR spectra of PCL-OH (a) and diblock copolymer PCL-*b*-PDMAEMA (b).

Polymeric Micelles Study. Critical micelle concentration (CMC) was commonly considered as an effective measure to evaluate the physical properties of micelles and the micelle stability. CMC was monitored by fluorimetry in the presence of pyrene as a hydrophobic fluorescent probe. Since pyrene is sensitive to polarity of the microenvironment, a dramatic decline of I_{339}/I_{335} could be found when it was transferred from polar solvent (*i.e.* water) to such non-polar environments as interior compartment of aggregates, self-assmbly of amphiphilic polymers in water. Thus the CMC value of polymer sample could be determined the moment pyrene entered into the hydrophobic core of the micelles. And in general, the CMC value of block copolymer was related closely to the proportion of different monomer-containing blocks, *i.e.*, the length ratio of hydrophilic blocks and hydrophobic ones on amphiphilic block copolymer. More hydrophobic modules with respect to hydrophilic segments would benefit the formation of polymeric micelles, resulting in thermodynamically stable assemblies with relatively low CMC value. To evaluate the impact of length of hydrophilic block on CMC value of copolymer, polymer samples were prepared (PCL_{50}-*b*-$PDMAEMA_{68}$, PCL_{50}-*b*-$PDMAEMA_{89}$, PCL_{50}-*b*-$PDMAEMA_{112}$) with molecular weight and molecular weight distribution as illustrated in Table 2, and the CMC value of each was determined by pyrene probe method respectively. As shown in Figure 4, the ratio of I_{339} to I_{335} varied in response to different copolymer concentrations, and the CMC value of amphiphilic copolymer was 0.012 mg/mL, 0.025 mg/mL and 0.037 mg/mL for PCL_{50}-*b*-$PDMAEMA_{68}$, PCL_{50}-*b*-$PDMAEMA_{89}$, PCL_{50}-*b*-$PDMAEMA_{112}$ according to methods described in experimental part. It can be found that with hydrophilic block (PDMAEMA) increasing, CMC value of the polymer sample increased accordingly. The result indicated that the ability of the samples with enhanced PDMAEMA:PCL to form micelles was impaired, which conformed with the conclusion of general studies. However, it is obvious that all the samples above showed an appreciable CMC value with the same order, suggesting a negligible discrepancy between them. Herein, the sample (PCL_{50}-*b*-$PDMAEMA_{89}$) which possessed medium length of hydrophilic blocks was selected for further

Table 2. Results of block copolymers

Sample	Time (min)	$Mn_{(th)}$[a] (g/mol)	$Mn_{(NMR)}$[b] (g/mol)	$Mn_{(GPC)}$[c] (g/mol)	Mw/Mn[c]
PCL_{50}-$PDMAEMA_{68}$	120	17300	17476	12600	1.30
PCL_{50}-$PDMAEMA_{89}$	180	21600	20773	15400	1.27
PCL_{50}-$PDMAEMA_{112}$	240	22527	24289	17527	1.32

[a]The theoretical molecular weights (Mn.th) calculated from the ratio of the initial monomer concentration to the initial initiator concentration $[M]_0/[I]_0$. [b]Determined by ^{1}H-NMR analysis. [c]Determined by GPC measurements.

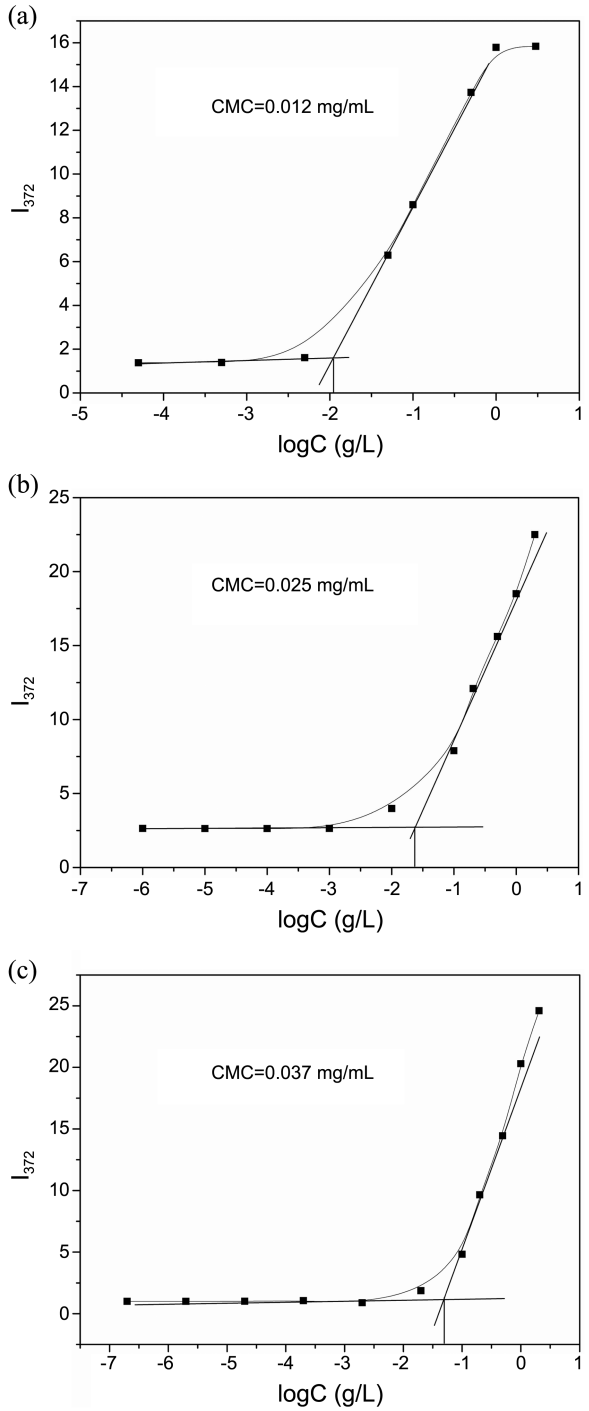

Figure 4. Plot of intensity versus logC for PCL-*b*-PDMAEMA. (a) PCL_{50}-*b*-$PDMAEMA_{68}$. (b) PCL_{50}-*b*-$PDMAEMA_{89}$. (c) PCL_{50}-*b*-$PDMAEMA_{112}$.

experiment.

Figure 5 showed the temperature and pH dependence of hydrodynamic diameter (Dh) of PCL-*b*-PDMAEMA micelles. With increasing temperatures from 25 to 60 °C, water progressively became a poor solvent for PDMAEMA blocks so that the stretched PDMAEMA chains collapsed onto the core, which led to a fierce decrease of Dh from 196 to 49.9 nm (Figure 5(a)). When the temperature rose up to 45 °C,

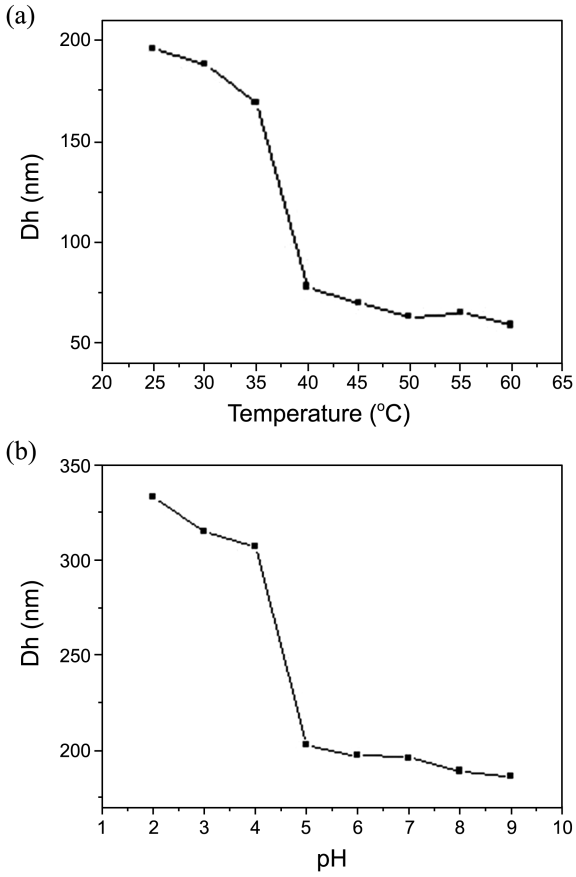

Figure 5. Temperature and pH dependence of hydrodynamic diameter (Dh) of PCL-*b*-PDMAEMA micelles measured at scattering angle 90°.

Dh approached a constant value indicating that the shrinkage of PDMAEMA blocks ceased and the structure of micelles formed. PDMAEMA was well known to be pH sensitive at aqueous solution, on account of the tertiary amine groups, which can be protonated and de-protonated under various pH conditions. pH reliance of the hydrodynamic diameter Dh of the micelles at different pH was shown in Figure 5(b). It was clear that Dh of the micelles increased abruptly with the decrease of pH values ranging from 5.0 to 4.0. The mean size of PCL-*b*-PDMAEMA nanoparticles increased from 186 nm to 335 nm when the pH decreased from 9.02 to 2, due to that the degree of protonation of tertiary amine groups of PDMAEMA chains was higher than that at a higher pH, and the hydrophilic shells of the micelles exhibited stronger electrostatic positive charge repulsion, which extended the chains of micellar shell and as a result the corresponding micelles took a larger size. However, at a higher pH, the micelles experienced the deionization of DMAEMA, which caused a de-swollen polymeric micelle and a smaller size.

In previous studies, TEM was used as a common tool to characterize morphologies of both blank and drug-loaded micelles. However, few reports were reported to focus on tapping-mode atomic force microscope. In comparison with TEM analysis, atomic force microscopy imaging demonstrates unique advantages to study the micelles with various

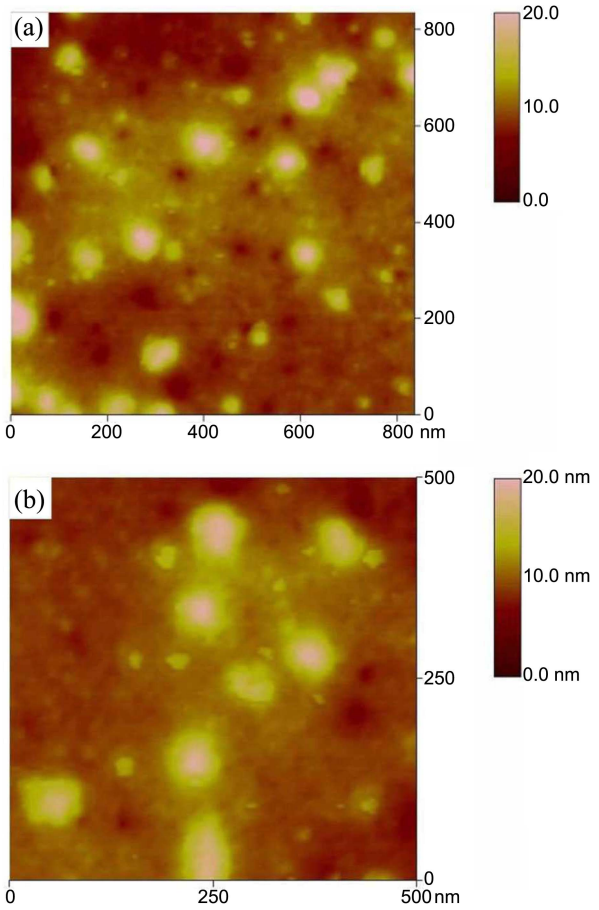

Figure 6. AFM image of blank micelles (a) and drug-loaded micelles (b) obtained from PCL-*b*-PDMAEMA.

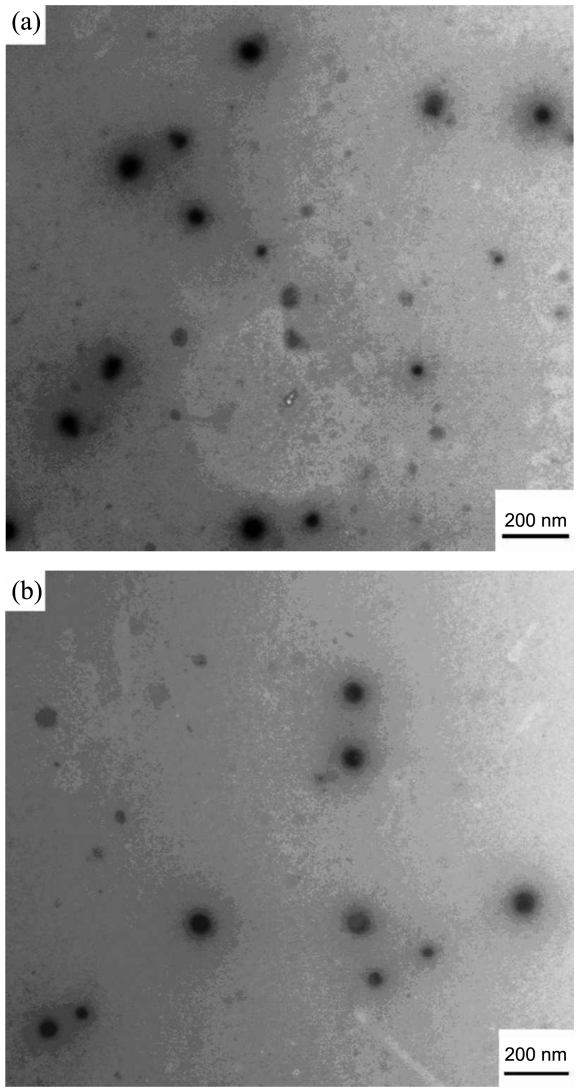

Figure 7. TEM image of blank micelles (a) and drug-loaded micelles (b) obtained from PCL-*b*-PDMAEMA.

morphologies. It does not need staining or coating of Pd/Pt alloy, thereby reducing the possibility of the aggregate deformation. Figure 6 showed the AFM images of the blank micelles (a) and drug-loaded micelles (b), which indicated that the self-assembled micelles were well dispersed as individual nanoparticles with a regularly spherical shape and the average diameters of blank micelles (a) and drug-loaded micelles were around 72 ± 20 nm and 78 ± 20 nm, respectively. There was no significant difference in particle morphologies and size of these two micelles, thus the observed difference in drug release behaviors of these two micelles may be attributed to other factors rather than micelle size or morphology. In addition, we all knew that spherical micellar nanoparticles (below 200 nm) will play an important role in drug delivery system in human interior tiny environment.

TEM was also performed to investigate the morphologies of the micelle and drug-load micelle as illustrated in Figure 7. TEM images seemed to follow the same trends as AFM results, both blank and drug-loaded micelles were generally spheroidal and no drug crystal was visible. The sizes (from TEM) for two kind micelles were approximately (75 ± 10 nm and 80 ± 10 nm, respectively). In addition, the hydrodynamic diameter values obtained from DLS studies were larger than those observed with AFM and TEM. The reason for this discrepancy might be that the micelles were swollen in solutions during the DLS measurements, whereas AFM and TEM showed the diameter of the dried aggregates.

pH is an important factor for drug delivery systems, due to the pH change occurs at many specific or pathological body sites, such as blood vessels, stomach, intestine, and tumor extracellular sites. Figure 8 showed the time dependence of cumulative paclitaxel release from drug-loaded micelles into buffer solutions at different pH at 37 °C. At pH 3, the common release profile with higher release rate and high total drug release (more than 86%) was observed. However, when the drug-loaded micelles solution was placed in pH 7.49 buffers at 37 °C, only 58% of the loaded drug can be released even after 72 h. This is due to the fact that the PDMAEMA shell was highly ionized and formed a stretched conformation at pH 3, and while as the pH increased from pH 4, flexibility caused by the decrease in degree of ionization or by the electrostatic screening effects was strengthened. Lower pH value rendered the PDMAEMA chain more hydrophilic, and facilitated the release of paclitaxel from the loosen micellar

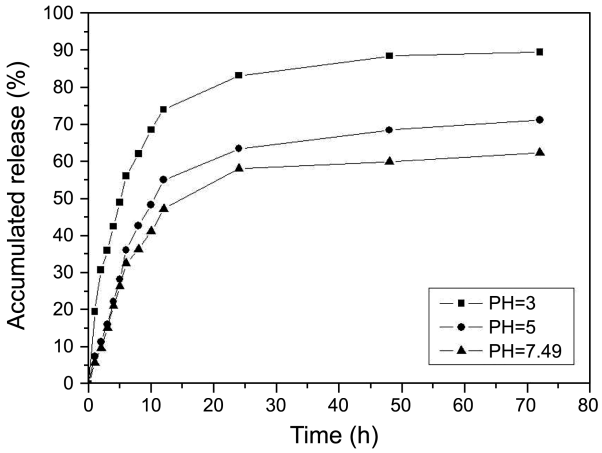

Figure 8. The pH-dependant drug release from the nanoparticles at 37 °C in PBS.

core due to the ionization of the PDEAEMA block, thus drug release rate in acid pH is much quicker than that in normal pH.

Temperature is one of the most widely used stimuli for stimuli-sensitive drug delivery system, because it is easy to control and has practical advantages both *in vitro* and *in vivo*. The cumulative release profiles of paclitaxel with various temperatures at pH 7.4 were investigated, as shown in Figure 9, an initial burst was observed with all the buffers within the first 5 h. The reason might be the localization of a little portion of paclitaxel in the outer shell or interfaces between the inner core and outer shell of the micelles. Moreover, the release rate of paclitaxel varied with the different temperatures in released solution. According to Figure 9, the amount and percentage of paclitaxel release is fastest at 41 °C, and then 39 °C, the least release rate was 37 °C. This could be explained by the deformations effect of the stable micelles, which was induced by the conformational transition of PDMAEMA segments, from extended hydrophilic chains to shrunk coils.

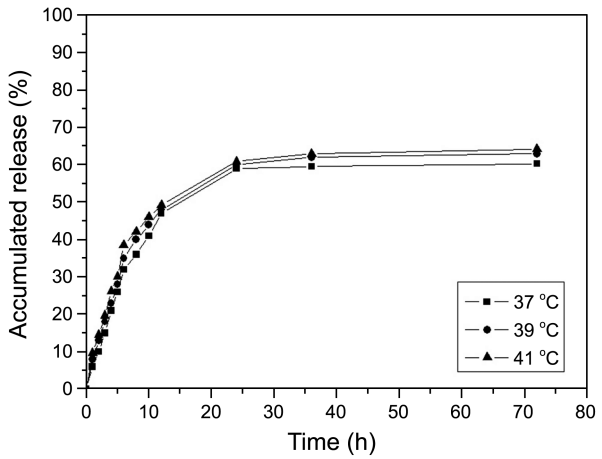

Figure 9. The temperature-dependant drug release from the nanoparticles in PBS.

Conclusion

In summary, well-defined amphiphilic block copolymers PCL-*b*-PDMAEMA were synthesized by combining eROP of -CL and ATRP of DMAEMA. The block copolymer could self-assemble into core-shell micelles in an aqueous media. AFM and TEM analysis of the micelles revealed their homogeneous spherical morphology with narrow size distribution. The drug release properties of the micelles were observed at different pH and temperature, and it was found that the influence of pH on drug release rate extremely was intense, whereas the release rate only exhibited a slight dependence on temperature. So the micelles had potential in drug delivery applications as well as the relevance of these developments to the field of biomedical research. Furthermore, in vivo pharmacokinetics and pharmacodynamics of this drug vehicle is still undergoing.

Acknowledgments. We are grateful to the Natural Science Foundation of P. R. China for the support of this work (no. 20574028). and Natural Science Foundation for youth for providing support. And the publication cost of this paper was supported by the Korean Chemical Society.

References

1. Adam, W.; Stacey, E.; Charles, L. *Adv. Drug. Delivery. Rev.* **2008**, *60*, 1018.
2. Mertoglu M.; Garnier S.; Laschewsky A. *Polymer* **2005**, *46*, 7726.
3. Tonhauser, C.; Golriz, A. A.; Moers, C. *Adv. Mater.* **2012**, *24*, 5559.
4. Ray, J. G.; Naik, S. S.; Hoff, E. A. *Macromol. Rapid Commun.* **2012**, *33*, 819.
5. Ganta, S.; Devalapally, H.; Shahiwala, A. *J. Controlled Release*. **2008**, *126*, 187.
6. Nishiyama, N.; Bae, Y.; Miyata, K. *Drug Discovery Today: Technologies* **2005**, *2*, 21.
7. Gao, Z.; Eisenberg, A. *Macromolecules* **1993**, *26*, 7353.
8. Meng, F.; Zhong, Z.; Feijen, J. *Biomacromolecules* **2009**, *10*, 197.
9. Zhang, W.; Shi, L.; Ma, R. *Macromolecules* **2005**, *38*, 8850.
10. Hu, Z.; Xia, X. *Adv. Mater*. **2004**, *16*, 305.
11. Isojima, T.; Lattuada, M.; Alan Hatton, T. *ACS Nano* **2008**, *2*, 1799.
12. Plamper, F. A.; Ruppel, M.; Müller, A. H. E. *Macromolecules* **2007**, *40*, 8361.
13. WellsF, A. *Org. Process Res. Dev.* **2006**, *10*, 681.
14. Scarpello, J. T.; Nair, D.; Freitas dos Santos, L. M. *J. Membr. Sci.* **2002**, *203*, 71.
15. Torque, C.; Bricout, H.; Hapiot, F. *Tetrahedron* **2004**, *60*, 6487.
16. López-Gallego, F.; Betancor, L.; Hidalgo, A. *J. Biotechnol*. **2004**, *111*, 219 .
17. Van Beilen, J. B.; Li, Z. *Curr. Opin. Biotechnol.* **2002**, *13*, 338.
18. Murakami, Y.; Hoshi, R.; Hirata, A. *J. Mol. Catal. B: Enzym.* **2003**, *22*, 79.
19. Ivanov, A. E.; Edink, E.; Kumar, A. *Biotechnol. Progr.* **2003**, *19*, 1167.
20. Konwarh, R.; Kalita, D.; Mahanta, C. *Appl. Microbiol. Biotechnol.* **2010**, *87*, 1983.
21. Yoshida, T.; Seno, K. I.; Kanaoka, S. *J. Polym. Sci., Part A: Polym. Chem.* **2005**, *43*, 1155.
22. Aoshima, S.; Sugihara, S.; Shibayama, M. *Macromol. Symp.* **2004**, *215*, 151.
23. Aoshima, S.; Sugihara, S. *J. Polym. Sci., Part A: Polym. Chem.* **2000**, *38*, 3962.
24. Ruckenstein, E.; Zhang, H. M. *Macromolecules* **1998**, *31*, 9127 .

25. Hirao, A.; Hayashi, M.; Haraguchi, N. *Macromol. Rapid Commun.* **2000**, *21*, 1171.
26. Hirao, A.; Higashihara, T.; Inoue, K. *Macromolecules* **2008**, *41*, 3579.
27. Cunningham, M. F. *Prog. Polym. Sci.* **2008**, *33*, 365.
28. Matyjaszewski, K.; Spanswick, J. *Materialstoday* **2005**, *8*, 26.
29. Yamago, S.; Iida, K.; Yoshida, J. I. *J. Amer. Chem. Soc.* **2002**, *124*, 2874.
30. Coessens, V.; Pintauer, T.; Matyjaszewski, K. *Progress in Polymer Science* **2001**, *26*, 337.
31. Tsarevsky, N. V.; Matyjaszewski, K. *Chem. Rev.* **2007**, *107*, 2270.
32. Licciardi, M.; Tang, Y.; Billingham, N. C. *Biomacromolecules* **2005**, *6*, 1085.
33. Li, C. Z.; Benicewicz, B. C. *Macromolecules* **2005**, *38*, 5929.
34. Lowe, A. B.; McCormick, C. L. *Prog. Polym. Sci.* **2007**, *3*, 283.
35. Cho, J. C.; Cheng, G. L.; Feng, D. S. *Biomacromolecules* **2006**, *7*, 2997.
36. Prabaharan, M.; Grailer, J. J.; Pilla, S. *Biomaterials* **2009**, *30*, 6065.
37. Blanazs, A.; Armes, S. P.; Ryan, A. J. *Macromol. Rapid Commun.* **2009**, *30*, 267.
38. Kwon, G. S.; Forrest, M. L. *Drug Dev. Res.* **2006**, *67*, 15.
39. Meyer, U.; Palmans, A. R. A.; Loontjens, T. *Macromolecules* **2002**, *35*, 2873.
40. Sha, K.; Qin, L.; Li, D. S. *Poly Bull.* **2005**, *54*, 1.
41. Sha, K.; Li, D. S.; Li, Y. P. *Macromolecules* **2008**, *41*, 361.
42. Wang, W.; Li, Y. P.; Zhao, Y. L. *Acta Polymerica Sinica* **2010**, *2*, 199.